Eur. Phys. J. A **31**, 566–571 (2007)
DOI 10.1140/epja/i2006-10178-5

THE EUROPEAN PHYSICAL JOURNAL A

Special Article – QNP 2006

Structure functions at HERA

D.H. Saxon[a]

Faculty of Physical Sciences, University of Glasgow, Glasgow, G12 8QQ, UK

Received: 24 September 2006
Published online: 16 February 2007 –

Abstract. HERA provides the key facility for the measurement of proton structure functions. Formalism and methods are outlined for the measurement and interpretation of inclusive structure functions, including the use of polarised $e^{\pm}$ beams. The measurement of charm, beauty and photon structure functions is discussed, together with special runs at low proton energy for measurement of the longitudinal structure function. Finally, the functions accessed using polarised beams on polarised targets are indicated.

PACS. 13.60.-r Photon and charged-lepton interactions with hadrons – 13.88.+e Polarisation in interactions and scattering – 14.65.-q Quarks – 14.70.Dj Gluons

1 Introduction

Deep inelastic scattering of $e^{\pm}$ on protons takes place via the exchange of a gauge boson, either neutral-current, (NC: γ or Z^0 exchange), or charged-current (CC: $W^{\pm}$ exchange, in which case the outgoing lepton is a neutrino or antineutrino). Defining k and k' as the incident and outgoing lepton four-momenta, then the exchanged boson carries four-momentum $q = k - k'$. We define the $Q^2 = -q^2 = -(k - k')^2$. If the incident proton four-momentum is p, then the centre-of-mass energy squared, $s = (p + k)^2 = 4E_eE_p$ (neglecting the rest masses). For 27.5 GeV $e^{\pm}$ incident on 920 GeV protons, $s = 101200\,\mathrm{GeV}^2$ and the c.m. energy is 318 GeV. When $Q^2 \simeq 0$ the exchanged photon is quasi-real and the process is refered to as photoproduction. The allowed range is $0 < Q^2 < s$. For virtual photons $Q^2 \neq 0$ and the process is called deep inelastic scattering (DIS).

The reaction is seen as a hard collision between the exchanged boson and a parton within the proton carrying a fraction $x = Q^2/2p \cdot q$ of the proton's momentum. x lies between 0 and 1, and the distribution of partons as a function of x is unknown *a priori*, although its evolution as a function of Q^2 is predicted [1]. The final state in lowest order contains an outgoing lepton, a jet from the struck parton and a forward-going proton remnant.

It is useful to introduce the quantity $y = p \cdot q/p \cdot k$. Then $y = \sin^2\theta/2$, where θ is the scattering angle in the lepton-parton centre of mass. Distributions in y are therefore influenced by the helicity structure of the process. Note that $0 < y < 1$ and that $Q^2 = sxy$.

[a] e-mail: d.saxon@physics.gla.ac.uk

For unpolarised $e^{\pm}p$ NC DIS the differential cross-section is given by

$$\frac{\mathrm{d}^2\sigma}{\mathrm{d}x\mathrm{d}Q^2} = \frac{2\pi\alpha^2}{xQ^4}\left[Y_+F_2(x,Q^2) - y^2F_L(x,Q^2) \mp Y_-xF_3(x,Q^2)\right],$$

where $Y_{\pm} = 1 \pm (1-y)^2$. The structure functions, F_i, are interpreted in terms of the quark $(q, \overline{q})$, and gluon (g), parton structure at a given (x, Q^2) as follows:

- $F_2 \simeq \Sigma x(q + \overline{q})$: dominates;
- $xF_3 \simeq \Sigma x(q - \overline{q})$: contributes at high Q^2;
- $F_L \simeq \alpha_s xg$: contributes at high y, absent in zeroth order QCD.

Thus measurement of the DIS rate gives direct sensitivity to quark distributions but only indirect sensitivity to gluons —F_L contributes typically a few percent at the highest y-bins. Gluons in the proton are accessed via the Q^2 evolution ($\mathrm{d}F_2/\mathrm{d}\ln Q^2$) or through measurements of the dijet rate, caused by photon-gluon fusion, $\gamma^*g \to q\overline{q}$, where the gluon is part of the incident photon structure (as well as by hard gluon bremsstrahlung from outgoing quarks, $\gamma^*q \to qg$).

The precision measurement of structure functions is interesting in its own right, and also provides the input needed for the calculation of every hard process at the LHC. All such interpretations of data at LHC will depend on the accuracy achieved at HERA.

2 Measurement of F_2 and parton densities

F_2 has been measured over the range ($0.00005 < x < 1$, $0.5 < Q^2 < 30000$) using NC data. (See fig. 1.) As

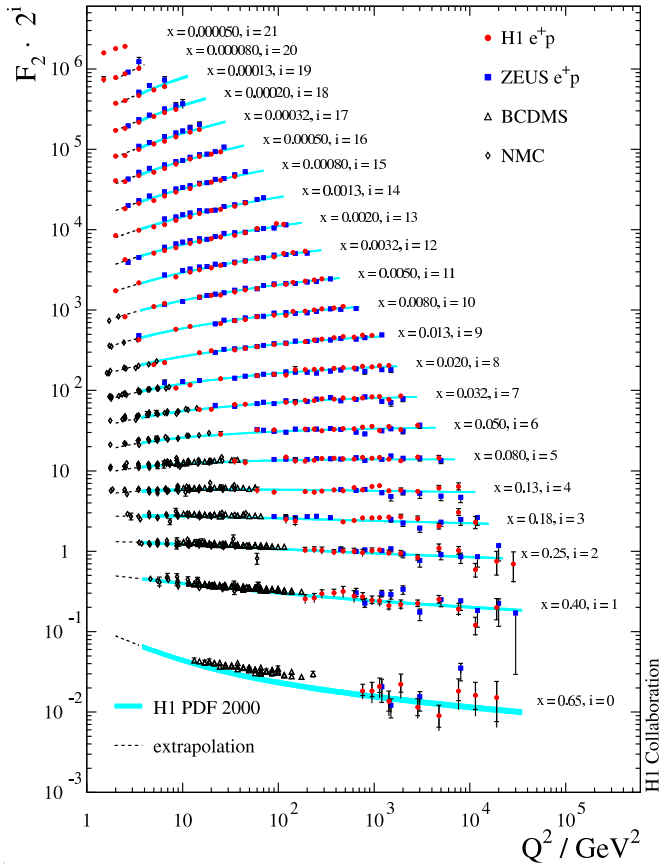

Fig. 1. Measurements of F_2.

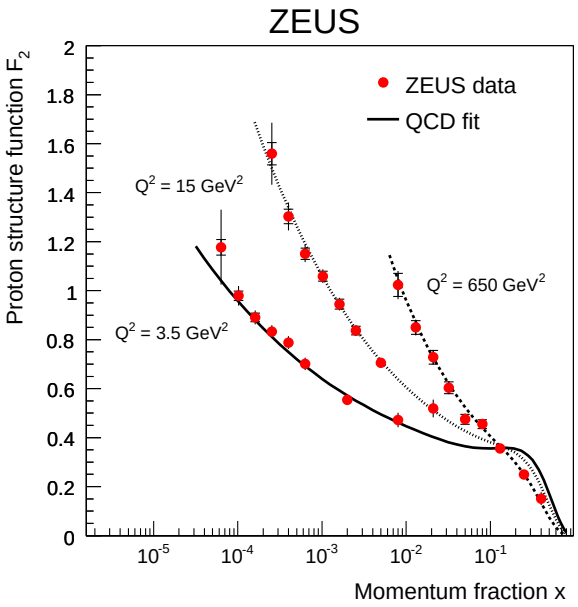

Fig. 2. Low-x behaviour of F_2 at different values of Q^2.

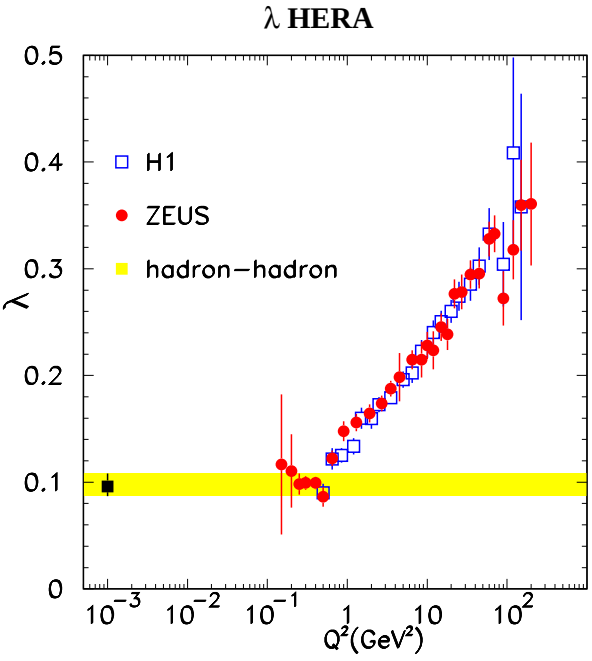

Fig. 3. Power λ for $F_2 \simeq x^{-\lambda}$ low-x fit.

a function of Q^2, F_2 falls for $x > 0.15$ and rises steeply for $x < 0.01$. (See fig. 2.) The high-x shape relates to the valence quark structure of the proton. At low x we are observing the universal structure of QCD radiation: at fixed Q^2 and low x, $F_2(x, Q^2) \simeq x^{-\lambda}$, with λ varying linearly with $\log Q^2$ from 0.1 for $Q^2 = 1$ to 0.35 for $Q^2 \simeq 100\,\mathrm{GeV}^2$. (See fig. 3.)

The full NC plus CC data set can be fitted to parametric forms to extract valence quark $(u_v(x), d_v(x))$ sea quark and gluon distributions at a reference value of $Q^2 = 10\,\mathrm{GeV}^2$. The 11-parameter analytic fit imposes factors such as the total number of valence quarks. The small F_L effects are input from NLO DGLAP calculations. For the reasons stated above the gluon distributions are relatively poorly determined. ZEUS have therefore made a combined fit to DIS rates and to dijet data [2]. This leads to reduced errors on fitted gluon distributions (see fig. 4) and to a major improvement in precision on α_s:

$$\alpha_s(M_Z) = 0.1183 \pm 0.0007(\mathrm{stat}) \pm 0.0027(\mathrm{syst}) \\ \pm 0.0008(\mathrm{model}) \pm 0.005(\mathrm{theory})$$

to be compared to the 2004 world average value, 0.1182 ± 0.0027. This measurement was made using data from one experiment alone. A study by the same authors of combining results from H1 and ZEUS showed movements outside the errors if the two data sets are simply combined. Care is needed, therefore, over systematic error estimates [1].

HERA II has now provided high statistics for both e^+p and e^-p. This permits extraction of xF_3 from the differences between the two data sets. The xF_3 NC term arises from the interference of γ and Z^0 exchange and hence is significant at high Q^2. Figure 5 shows early HERA II results.

3 Charged current results

HERA has now delivered over $200\,\mathrm{pb}^{-1}$ of e^-p data, including beam polarisations of $+32\%$ and -41%. The rest

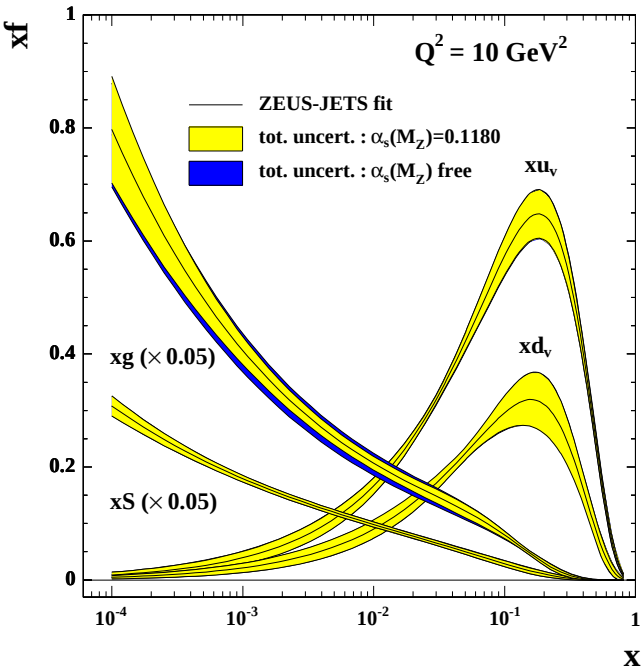

Fig. 4. Fitted parton distributions in the ZEUS jets fit.

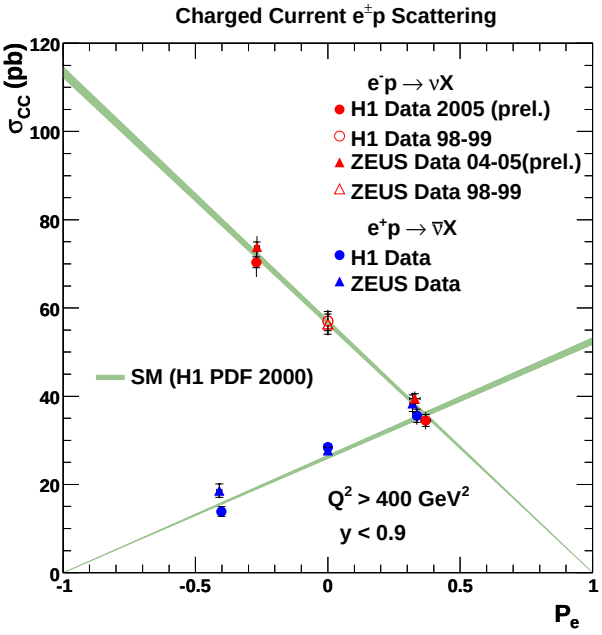

Fig. 6. The linear dependence of charged-current cross-sections on lepton beam polarisation.

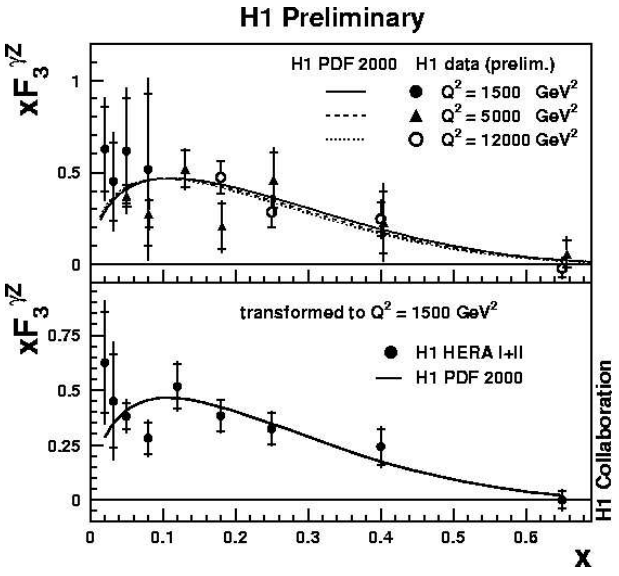

Fig. 5. xF_3 from differences of e^+p: 150 pb^{-1} and e^-p: 135 pb^{-1} data.

of the running will be for e^+p (where polarisations of +33% and −27% have been achieved). The high luminosity allows us to access high-statistics CC data. The CC cross-sections are sensitive to quark and antiquark flavours as follows:

$$\frac{\mathrm{d}^2\sigma}{\mathrm{d}x\mathrm{d}Q^2}(e^+p) = \frac{G_F^2}{2\pi x}\frac{M_W^4}{(Q^2+M_W^2)^2}x[\overline{u}+\overline{c}+(1-y)^2(d+s)],$$

$$\frac{\mathrm{d}^2\sigma}{\mathrm{d}x\mathrm{d}Q^2}(e^-p) = \frac{G_F^2}{2\pi x}\frac{M_W^4}{(Q^2+M_W^2)^2}x[u+c+(1-y)^2(\overline{d}+\overline{s})],$$

where the quark flavour distributions are functions of x and Q^2. Both e^+p and e^-p are needed to separate the different quark flavours. Running at positive and negative beam helicities will assist this activity.

The first step in this process is to verify the helicity dependence of the cross-section. For pure $W^\pm$ exchange we expect

$$\sigma_{CC}^{e^\pm p}(P_e) = (1 \pm P_e)\sigma_{CC}^{e^\pm p}(P_e = 0).$$

Figure 6 shows a standard model fit to the data, with zero intercepts at $P_e = \pm 1$ [3]. This is a good fit to the data and so there is no need for W_R exchange and we can set lower limits on the W_R mass (for standard couplings) of order 200 GeV. Bin-by-bin comparisons of $\sigma(RH)/\sigma(LH)$ show Q^2-dependence consistent with the standard model.

Polarised data also allow us to extract the vector and axial weak couplings of the u and d quarks. Precisions are comparable to measurements at LEP and resolve the LEP sign ambiguity (where only the sign of the product of vector and axial couplings is measured).

4 Heavy flavour production

Charm and beauty production NC cross-sections are used to define structure functions as follows (ignoring xF_3 for moderate Q^2):

$$\frac{\mathrm{d}^2\sigma}{\mathrm{d}x\mathrm{d}Q^2}(c\overline{c}) = \frac{2\pi\alpha^2}{xQ^4}[Y_+F_2^{c\overline{c}} - y^2F_L^{c\overline{c}}]$$

and similarly for b-production. Production is dominated by photon-gluon fusion. Both ZEUS and H1 have operational vertex detectors. Results are available using vertex

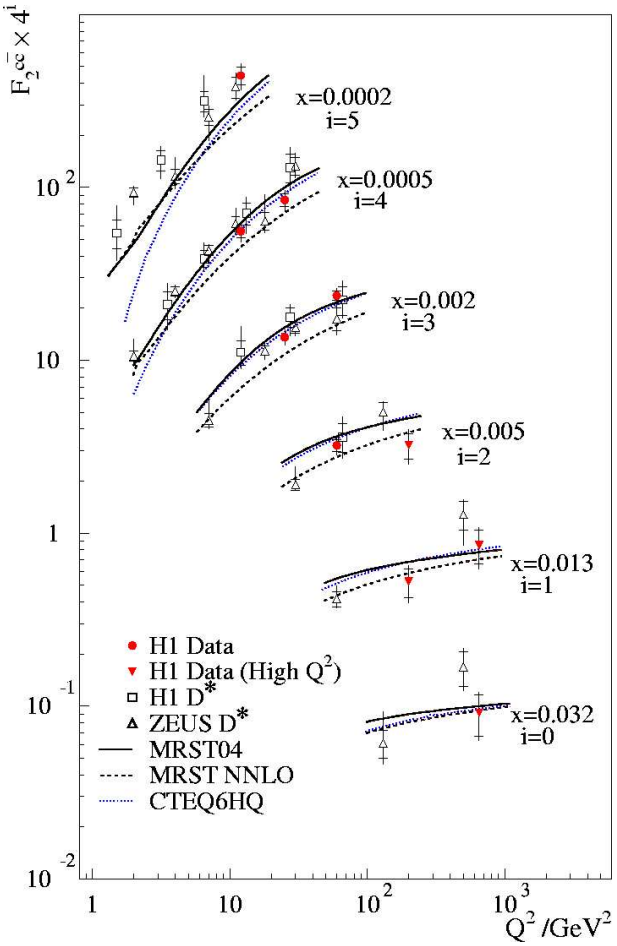

Fig. 7. Charm structure functions from vertex and $D^{*\pm}$ tagging.

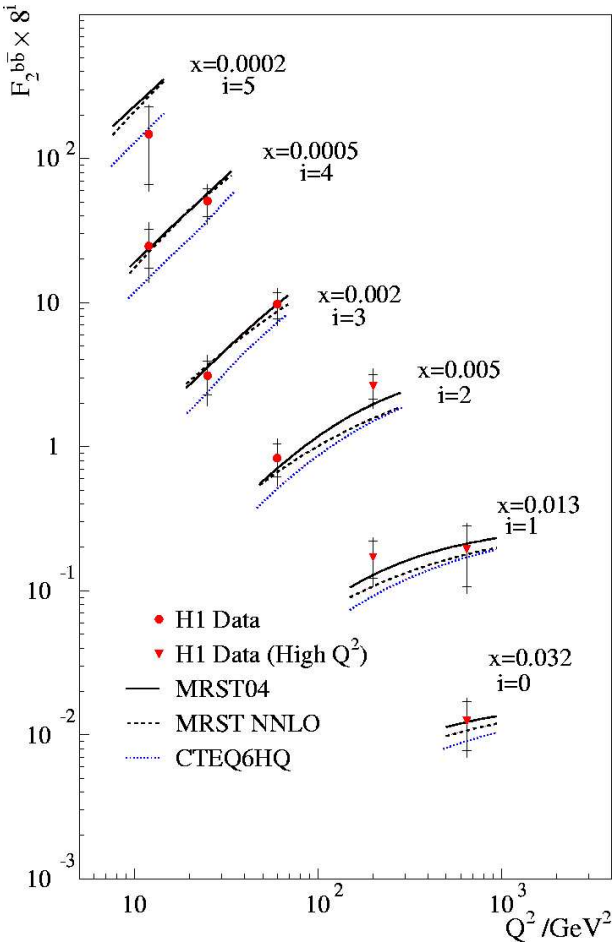

Fig. 8. Beauty structure functions from vertex tagging.

detector decay time tagging in H1 [4]. The detector acceptance is good at modest laboratory rapidity, providing measurements for $0.0002 < x < 0.032$ and Q^2 up to $650\,\mathrm{GeV}^2$.

The H1 vertex detector provides trajectory measurements with accuracy $\sigma_{r\phi} = 12\,\mu$m, $\sigma_z = 25\,\mu$m at 5.7 cm radius. Tracks are extrapolated back to the primary production vertex. The miss distance (called the impact parameter, δ) arises from measuring error (positive or negative) or from parent flight before decay. $\delta \simeq 0.7c\tau$, so a b lifetime of 1.5 ps gives a mean impact parameter of $300\,\mu$m. We define the significance $S = \delta/\sigma(\delta)$. Raw data distributions are dominated by measuring error. Algorithms are devised using the second highest significance for charm and the third highest for beauty. The negative-S tail is subtracted from the positive data since the light-quark background is symmetric in S and this reduces the sensitivity to normalisation and to the knowledge of the resolution. Results are shown in figs. 7 and 8, together with earlier charm results based on $D^{*\pm}$ tagging. F_L corrections are about 3% at the highest y. Scaling violations are large, as expected for a gluon-driven process. Theoretical predictions for charm are rather different for NLO and NNLO. MRST and CTEQ agree with the charm results except at the lowest x and Q^2. Their predictions for beauty differ by a factor of two but the data errors are sufficiently large not to discriminate between them. Depending on x and Q^2, charm accounts for 15 to 30% of events and beauty for 0.3 to 3.5%. NLO QCD describes these ratios well.

5 Prompt photon production in deep inelastic scattering

Photons emitted at high E_T and well isolated in rapidity-azimuth space are regarded as arising from hard emission from an electron or quark line in the primary Feynman diagram and not as the secondary products of jet fragmentation. ZEUS data on inclusive prompt photons and photon-plus-jet disagreed with the predictions of different (divergent) Monte Carlo models and agreed only modestly with NLO calculations available at the time [5]. The process has two hard scales, Q^2 and E_T and NLO for photon-plus-jet is of order $(\alpha^3\alpha_s)$, so it is quite challenging to calculate.

This stimulated MRST to look at the process as the DIS of an electron off a photon which is itself a constituent of the photon, the electron emitting hard non-collinear bremsstrahlung [6]. Such constituent photons must be expected from the QED analogue of DGLAP evolution, and

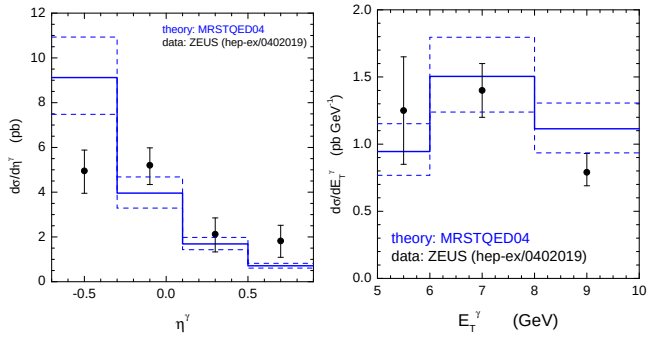

Fig. 9. Inclusive DIS prompt photon production compared to MRST predictions (absolute normalisation).

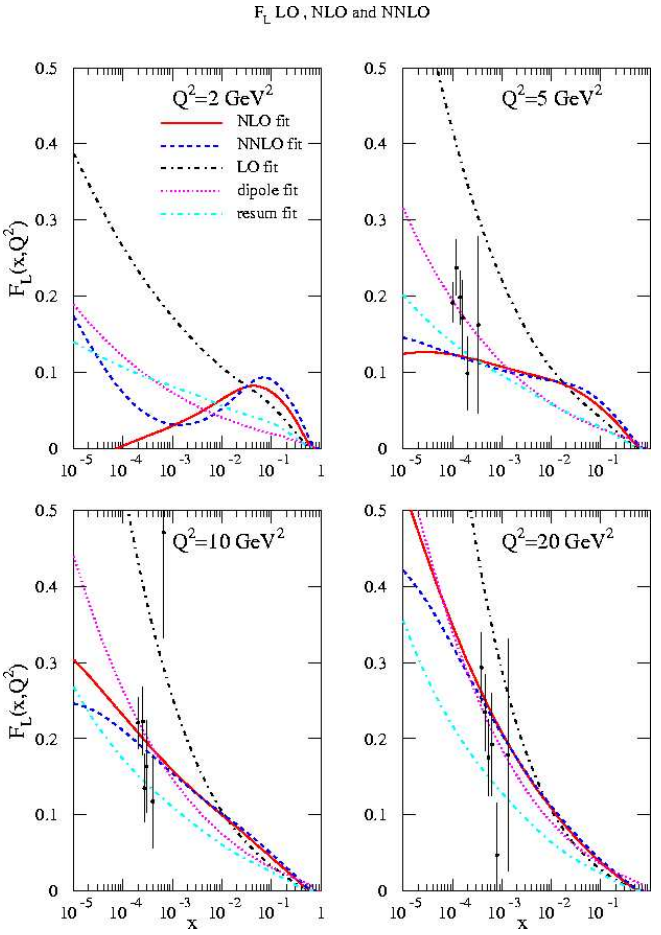

Fig. 10. Different theoretical predictions for F_L together with hypothetical measurements with errors of the expected size.

one can calculate a generated $F_2^\gamma(x, Q^2)$. Predictions for absolute rate, Q^2 distribution, photon E_T and rapidity are all close to the data, though the rapidity distribution in the data is flatter than the theory (see fig. 9) suggesting that a photon radiation from quarks needs to be added. Subsequent to this work, new NLO calculations for conventional DIS have been produced close to the ZEUS data and also to recent H1 results [7]. There is therefore not yet an integrated approach combining $F_2^\gamma(x, Q^2)$ with photon

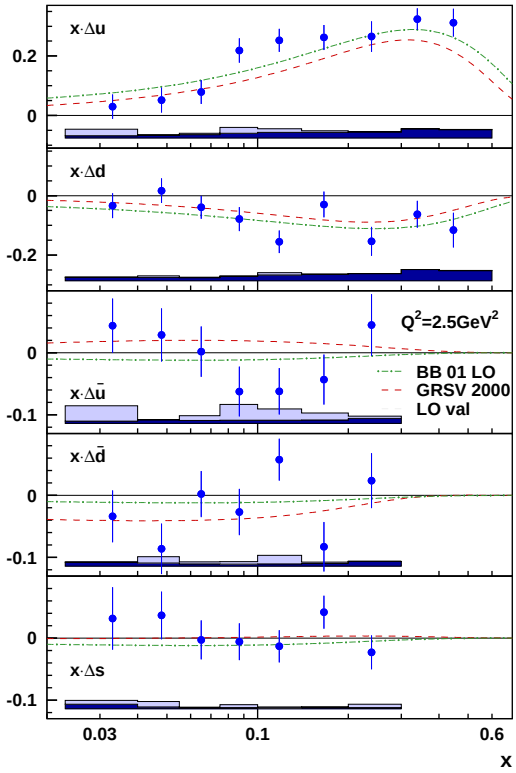

Fig. 11. HERMES measurements of nucleon longitudinal spin structure.

emission from quarks and jet production. Logically, this ought to exist.

6 Measurement of F_L

Extraction of F_L is difficult for several reasons. Recall we need high y to see its effect, which is normally only a few percent even then. Since $Q^2 = sxy$, at fixed x and Q^2 this means low s. Special runs have therefore been proposed for 2007 at reduced proton beam energy, for example three months at 50% of nominal beam energy. F_L is then extracted by comparing the same (x, Q^2) bins at different values of y. High y is experimentally quite challenging as it demands low outgoing electron energy, giving challenges to triggering, energy resolution and to backgrounds from photoproduction.

The present knowledge of F_L is scant and theories are divergent at low Q^2 and low x, due to large uncertainties in gluon distributions. There are major differences between LO, NLO and NNLO calculations [8] (see fig. 10). Measuring F_L is therefore both a test for perturbative QCD and a calibration for the LHC. $5\,\mathrm{pb}^{-1}$ of data at 460 GeV proton energy plus $3.5\,\mathrm{pb}^{-1}$ at 575 GeV give errors of order 0.05 to 0.1 (F_L is typically about 0.3) in a total of 18 (x, Q^2) bins.

7 Measurements with polarised targets

The HERMES experiment collides the electron beam with a proton target, either both polarised longitudinally or

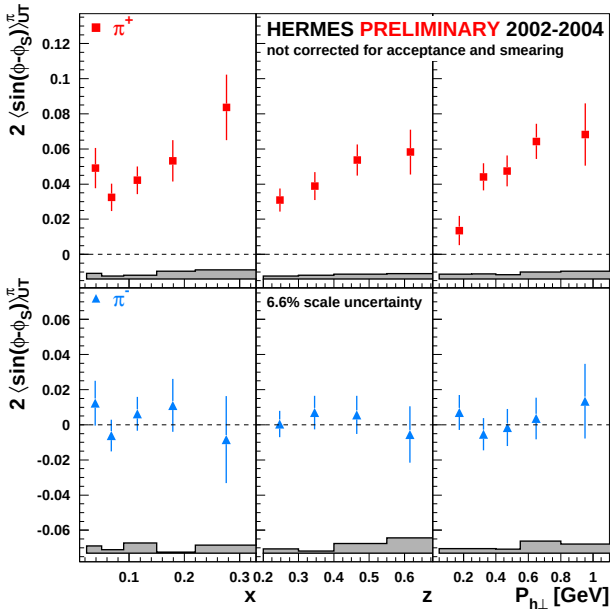

Fig. 12. Sivers moments for π^+ and π^- as a function of x, $z = E_{\rm hadron}/E_{\rm jet}$, and hadron transverse momentum $P_{h\perp}$.

unpolarised electron hitting transversely polarised proton. For a proton gas jet target $|P_z| \simeq 0.85$. The difference in rates for ep spins parallel or antiparallel allows us to access the spin structure of the proton. Choosing a proton with its spin pointing in the z-direction,

$$\left\langle S_z^N \right\rangle = \frac{1}{2} = \frac{1}{2}\Delta\Sigma + L_q + J_g \,,$$

$\Delta\Sigma$ here is the quark spin asymmetry. This should be 1 if all the proton spin is due to aligning the spin of the quarks. Other possible contributions arise from the orbital angular momentum of the quarks, L_q, or polarisation of the gluons, J_g. Events are flavour-tagged by identifying a leading $\pi^\pm$ or $K^\pm$. This allows decomposition of the spin asymmetry into $u, \overline{u}, d, \overline{d}$ and $(s + \overline{s})$ [9]. Figure 11 shows the results as a function of x. Integrating over the range $0.2 < x < 1$ HERMES find $\Delta\Sigma(u + \overline{u} + d + \overline{d}) = 0.286 \pm 0.026 \pm 0.011$, $\Delta\Sigma(s + \overline{s}) = 0.006 \pm 0.029 \pm 0.007$. $\Delta\Sigma(\overline{u}$ and $\overline{d})$ are consistent with zero with errors of 0.04. We note that there is no evidence for a large strange-quark component, but that more than half of the proton spin is unaccounted for.

This question is addressed by HERMES data taken using a transversely polarised proton target [10]. Take as the xz-plane the plane containing the incident and outgoing leptons with the exchanged photon along the z-axis. Let ϕ_s be the azimuthal angle of the target spin polarisation in this frame and ϕ be the azimuthal angle of the outgoing hadrons. The distributions in the Collins moments, $\langle \sin(\phi + \phi_s) \rangle$, and Sivers moments $\langle \sin(\phi - \phi_s) \rangle$, together with $\langle \sin(2\phi - \phi_s) \rangle$, and $\langle \sin(\phi_s) \rangle$ are measured. The Sivers moments are consistent with zero for outgoing π^- but significant for π^+. This results requires L_q to be non-zero (see fig. 12).

I thank the organisers for arranging this informative meeting, colleagues on HERMES, H1 and ZEUS for assistance and Chris Collins-Tooth for his comments and help.

References

1. Robin Devenish and Amanda Cooper-Sarkar, *Deep Inelastic Scattering* (Oxford University Press, New York, 2004).
2. ZEUS Collaboration (S. Chekanov *et al.*), Eur. Phys. J. C **42**, 1 (2005).
3. H1 Collaboration (A. Aktar *et al.*), Phys. Lett. B **634**, 173 (2006); ZEUS Collaboration, hep-ex/0602026.
4. H1 Collaboration (A. Aktar *et al.*), Eur. Phys. J. C **45**, 23 (2006).
5. ZEUS Collaboration (S. Chekanov *et al.*), Phys. Lett. B **595**, 86 (2004).
6. A.D. Martin *et al.*, Eur. Phys. J. C **39**, 155 (2005).
7. A. Gehrmann-De Ridder *et al.*, Phys. Rev. Lett. **96**, 132002 (2006). See also, hep-ph/0605222.
8. A.D. Martin, W.J. Stirling, R.S. Thorne, Phys. Lett. B **635**, 305 (2006).
9. HERMES Collaboration (A. Airepetian *et al.*), Phys. Rev. Lett. **92**, 012005 (2004).
10. HERMES Collaboration (A. Airepetian *et al.*), Phys. Rev. Lett. **94**, 012002 (2005).